

# Triacylglycerol Estolides, a New Class of Mammalian Lipids, in the Paracloacal Gland of the Brushtail Possum (*Trichosurus vulpecula*)

Stuart McLean<sup>1</sup> · Noel W. Davies<sup>2</sup> · David S. Nichols<sup>2</sup> · Bernie J. Mcleod<sup>3,4</sup>

Received: 27 January 2015 / Accepted: 14 April 2015 / Published online: 28 April 2015  
© AOCS 2015

**Abstract** The paracloacal glands are the most prevalent scent glands in marsupials, and previous investigation of their secretions in the brushtail possum (*Trichosurus vulpecula*) has identified many odorous compounds together with large amounts of neutral lipids. We have examined the lipids by LC–MS, generating ammonium adducts of acylglycerols by electrospray ionisation. Chromatograms showed a complex mixture of coeluting acylglycerols, with *m/z* from about 404 to 1048. Plots of single  $[M + NH_4]^+$  ions showed three groups of lipids clearly separated by retention time. MS–MS enabled triacylglycerols and diacylglycerol ethers to be identified from neutral

losses and formation of diacylglycerols and other products. The earliest-eluting lipids were found to be triacylglycerol estolides, in which a fourth fatty acid forms an ester link with a hydroxy fatty acid attached to the glycerol chain. This is the first report of triacylglycerol estolides in animals. They form a complex mixture with the triacylglycerols and diacylglycerol ethers of lipids with short- and long-chain fatty acids with varying degrees of unsaturation. This complexity suggests a functional role, possibly in social communication.

**Keywords** Triacylglycerol · Estolide · Diacylglycerol ether · LC–MS analysis · GC–MS analysis · Paracloacal scent glands · Brushtail possum · *Trichosurus vulpecula* · Pheromone · Marsupial

The number of carbon atoms and double bonds in fatty acids and acyl groups is indicated as Cn:x. The total number of radical (acyl or alkyl) carbons attached to glycerol for each lipid type is given with the total number of acyl double bonds, e.g. TAG 30:1, DAGE 31:1, EST 50:3. The fatty acid composition is shown as a list which does not specify the *sn*-positions, e.g. 7:0/9:0/17:0. The alkyl substituent in DAGE is marked with the ether link, e.g. 7:0/7:0/e16:0. The fourth acyl substituent in TAG-estolides is similarly indicated as 7:0/7:0/h18:1–18:2.

**Electronic supplementary material** The online version of this article (doi:10.1007/s11745-015-4025-9) contains supplementary material, which is available to authorized users.

✉ Stuart McLean  
stuart.mclean@utas.edu.au

<sup>1</sup> Division of Pharmacy, School of Medicine, University of Tasmania, Private Bag 26, Hobart 7001, Australia

<sup>2</sup> Central Science Laboratory, University of Tasmania, Private Bag 74, Hobart 7001, Australia

<sup>3</sup> AgResearch, Invermay Agricultural Centre, Puddle Alley, Mosgiel 9053, New Zealand

<sup>4</sup> Present Address: Dukes Rd, RD 2, Mosgiel 9092, New Zealand

## Abbreviations

FA	Fatty acid(s)
<i>h</i> FA	Hydroxy fatty acid(s)
FAME	Fatty acid methyl ester(s)
TMS	Trimethylsilyl derivative
TAG	Triacylglycerol(s)
DAGE	Diacylglycerol ether(s)
EST	Estolide(s), an ester formed from a FA and an <i>h</i> FA; also the abbreviation for TAG-estolide
Lyso	Diacylglycerol product ion
NL	Neutral loss
GC–MS	Gas chromatography–mass spectrometry
LC–MS	Liquid chromatography–mass spectrometry
UPLC	Ultra high performance liquid chromatography
EI	Electron ionisation
ESI	Electrospray ionisation
RT	Retention time
ESM	Electronic supplementary material

## Introduction

The common brushtail possum, *Trichosurus vulpecula* (“possum”) is a cat-sized Australian marsupial, which is arboreal, nocturnal and solitary. It possesses several secretory glands which appear to be used for olfactory communication [1]. However, the composition of their secretions is only beginning to be characterised, and very little is known of their role in possum biology. The possum has two pairs of exocrine glands in the paracloacal wall, the more proximal producing an oily, odiferous secretion. Woolhouse *et al.* [2] found that the proximal glands contain a large number of triacylglycerols (TAG) which, on saponification, yield C7–C9 branched (*iso* and *anteiso*) fatty acids, as well as C14, C16 and C18 fatty acids. We have since extended this study, using swabs of the paracloacal region of possums, and confirmed the presence of these compounds as well as finding many additional fatty acids (from C4–C25), together with fatty alcohols and some unusual formate and dimethyloctyl esters and sulphur compounds [3]. Saponification of lipid extracts also produced some alkylglycerol ethers (C13–20), which were considered to have come from diacylglycerol ether (DAGE) parents, although no direct evidence of this was obtained. The present study has further investigated the lipids of possum proximal paracloacal glands. We have found that the glands contain a complex mixture of TAG and DAGE as well as triacylglycerol estolides, a new class of lipids not previously reported to occur in animals.

Acylglycerols typically comprise up to three acyl chains attached to the glycerol via individual ester linkages. When one of the acyl chains contains an hydroxyl group, this can be further esterified by another fatty acid forming an estolide (an ester formed from two fatty acids [4]). In this manner one or more fatty acids can be added to an acylglycerol, and such estolides have been reported in a number of plant species (reviewed by Lin *et al.* [5] and Smith *et al.* [6]). For example, castor (*Ricinus communis* L.) oil is mostly (70 %) triricinoleoylglycerol and, as ricinoleoleic acid is (*Z*,12*R*)-12-hydroxyoctadec-9-enoic acid, a small amount (0.5 %) of the triacylglycerol estolide (or tetraacylglycerol) has been found in castor oil [5]. Estolides can also comprise chains of multiple hydroxy fatty acids, as found in the seed oils of *Mallotus philippensis* and *Trewia nudiflora* which produce kamolenic acid (18-hydroxy-*cis*-9,*trans*-11,*trans*-13-octadecatrienoic acid) [6]. For example acylglycerols were found with seven fatty acids, five of which were in one position on the glycerol backbone. Tetraacylglycerols have also been found as minor components in the seed oil of lesquerella (*Physaria fendleri*), with estolide groups formed from lesquerolic acid ((*Z*,14*R*)-14-hydroxyicos-11-enoic acid) [7].

## Materials and Methods

### Animals

Possums of both sexes (11 females, 7 males) were live trapped and housed together with other possums in the AgResearch Brushtailed Possum Facility, Mosgiel, New Zealand. They were maintained under standard conditions and had full access to food and water [8]. The capture, housing and experimental procedures had prior approval by the AgResearch Invermay Animal Ethics Committee in accordance with the NZ Animal Welfare Act (1999). Possums were anaesthetised with halothane (Fluothane, ICI NZ Ltd, New Zealand) then killed by an intracardiac injection of pentobarbitone (Euthal, Delta Veterinary Laboratories, NSW, Australia). The proximal paracloacal glands were immediately removed and kept separately in glass vials with Teflon-sealed caps at  $-20^{\circ}\text{C}$ . The glands had a similar weight for females (mean  $1.13 \pm 0.34$  (SD) g,  $n = 11$ ) and males ( $1.05 \pm 0.40$  g,  $n = 7$ ). The glands were transported on dry ice to Hobart, Australia, for the chemical analyses and stored there at  $-80^{\circ}\text{C}$ . Samples of body fat (abdominal and renal) were obtained from an adult male Tasmanian possum which had been euthanased after road injury.

### Extraction of Lipids

Proximal paracloacal glands were thawed in the vial at room temperature, then placed on a piece of aluminium foil on a glass slab. An incision was made with a scalpel blade and the gland gently squeezed with forceps to produce the viscous, creamy and malodorous contents which were aspirated with a 200- $\mu\text{l}$  capillary pipette (Transferpette, Brand, Germany). About 100  $\mu\text{l}$  (approx. 100 mg) were placed in a tared 10-ml centrifuge tube, weighed, and diluted by vortex-mixing with  $2 \times 100 \mu\text{l}$  distilled water. This was extracted with 1 ml dichloromethane and this lipid extract was used for LC–MS and GC–MS analyses. Samples of abdominal and renal fat were crushed in liquid nitrogen and extracted with dichloromethane, then filtered before analysis by LC–MS, using a concentration of about 1 mg/ml. Other samples of body fat were saponified as described below, and the free fatty acids analysed as their methyl esters by GC–MS.

### GC–MS Analyses

Lipid extracts were analysed by GC–MS as previously described [3], except that the mass spectrometer was a Bruker 300-MS Triple Quadrupole instrument using electron ionisation (EI). A mix of alkane standards (C7–C40

in hexane; Supelco, USA) was added to some samples before GC–MS analysis for determination of Kovats Indices. The glycerides were investigated by selected ion chromatograms using the masses calculated for the diacyl product ions formed after the loss of an alkanolate group ( $[M - RCOO]^+$ ), as well as acyl-related ions ( $RCO^+$ ,  $[RCO - H_2O]^+$ ,  $[RCO + 74]^+$  [9]). Fatty acids, hydroxyl fatty acids and glycerol ethers were investigated after hydrolysis and derivatisation (see ESM).

### UPLC–MS Analyses

Lipid extracts were analysed using a Waters Acquity H-series UPLC coupled to a Waters Xevo triple quadrupole mass spectrometer. A Waters Acquity UPLC BEH C18 column ( $2.1 \times 100 \text{ mm} \times 1.7 \mu\text{m}$  particles) was used, with mobile phases comprising solvent A = 100 mM ammonium acetate, pH 5.0; solvent B = acetonitrile; and solvent C = methanol/hexane (80:20, by vol). The solvent gradient was: 100 % A/B (20:80, by vol) from 0 min to 100 % B at 2.0 min; followed by a linear gradient to 100 % C at 8 min; held for 14 min; returned to starting conditions over 1 min; then 3 min re-equilibration time. Flow rate was 0.5 ml/min for 2 min followed by an immediate ramp to 0.6 ml/min. A post-column addition of 3  $\mu\text{l}$  5 % (by vol) ammonia solution was added prior to the effluent entering the mass spectrometer. The mass spectrometer was operated in positive ion electrospray mode and several different full scans, product ion scans and parent ion scans were employed. The ion source temperature was 150 °C, the desolvation gas was nitrogen at 1000 l/h, the desolvation temperature was 300 °C and the capillary voltage was 2.8 kV.

Typical full scan acquisitions were over the range  $m/z$  100 to 1050 in 0.3 s, and were acquired at three different cone voltages (20, 45 and 70 V) in peak centroid mode. Targeted product ion scans were acquired from various precursor ions starting from 50  $m/z$  units above the precursor ion value down to  $m/z$  100 at a speed of 5000  $m/z$  units/s. Typically 4 precursor ions were selected to run in the same experiment. Cone voltage (CV) for these runs was 45 V and collision energy (CE) was 17 V, and the data were acquired in profile mode. Parent ion scans were acquired for  $m/z$  299 using two different settings for cone voltage and collision energy (25 CV, 17 CE and 40 CV, 30 CE), with simultaneous acquisition of normal full scan data. Pseudo ‘MS<sup>3</sup>’ experiments from a range of precursor ions including  $m/z$  449 were conducted by inducing in-source fragmentations with a cone voltage of 70 V and a collision voltage of 17 V, scanning at 5000  $m/z$  units/s.

The principal ions formed under the conditions used were the ammoniated parent lipids ( $[M + NH_4]^+$ ), although sodium adducts were also formed to a lesser extent and the ratio of these adducts depended strongly

on the electrospray cone voltage. MS–MS showed diacyl product ions (lyso ions) formed by the loss of RCOOH and  $NH_3$  from the  $[M + NH_4]^+$  ion. These neutral losses were used to identify the fatty acid chain size of the TAG and other lipids. Confirmatory ions were produced from the acyl fragments:  $[RCO]^+$ ,  $[RCO - 18]^+$  and, from the glycerol backbone,  $[RCO + 74]^+$  and its dehydrated form [10, 11]. As a reference standard, a mixture of TAG of five fatty acids (tricaprylin, tricaprillin, triaurin, trimyristin and tripalmitin) was obtained from Supelco (USA).

### Accurate Mass Measurements by LC–MS

Samples were separated using a Waters Novapak 4- $\mu\text{m}$  C18 column ( $3.91 \times 150 \text{ mm}$ ) at a flow rate of 0.8 ml/min, controlled by a Waters Alliance 2690 separation module. A linear gradient from 100 % solvent A (methanol with 0.1 % formic acid, by vol) to 100 % solvent B (methanol/hexane, 80:20, with 0.1 % formic acid, by vol) over 15 min was used, followed by 15 min hold of solvent B.

Mass spectral data was acquired using an LTQ-Orbitrap XL (Thermo Scientific, Australia) with electrospray ionisation (ESI) in positive ion mode. Full scan ( $m/z$  50–2000) spectra were acquired in profile mode at a resolution of 30,000. The ESI parameters used were: capillary temperature of 325 °C, spray voltage 4 kV and sheath gas and auxiliary gas 30 and 5 AU, respectively. This instrument did not allow ready post-column addition of an ammonia solution so generation of ammoniated ions was not pursued, and the sodiated species (generated without extra addition of any sodium ions) were measured instead.

### Search Strategy

The full scan LC–MS data were very complex, and single ion chromatograms were used to obtain retention times (RT) of individual masses. The full mass spectrum was inspected for each peak to exclude those due to isotope effects or noise. At higher masses the ion chromatograms tended to become more complex with greater numbers of isomers and broader peaks with multiple maxima. The RT was taken as either the highest peak, or the midpoint, as appropriate. Data from multiple ion chromatograms enabled regression plots of RT versus  $m/z$  which enabled lipids to be distinguished by structural group, carbon number and level of unsaturation.

## Results

### GC–MS Analyses

GC–MS analysis of total lipid extracts of proximal gland contents produced a large number of TAG molecular

species, many unresolved, which eluted towards the end of the temperature program (see Electronic Supplementary Material, ESM). Saponification showed that the TAG lipids were formed from at least 69 short- and long-chain fatty acids, from C6–C24, branched- and straight-chain, some unsaturated, but dominated by *iso*- and *anteiso*-isomers of heptanoic and nonanoic acid, which have been described previously [2, 3]. For each lipid peak, the parent TAG was reconstructed from the mass spectrum using the diagnostic EI fragment ions [9]. A common pattern was for isobaric TAG to elute as a set of three peaks, although each peak could include more than one molecular species. This occurred even when only one FA was present, for example TAG 7:0/7:0/7:0, probably due to the TAG being mixtures of *iso*-, *anteiso*- and *n*-isomers, with their different elution times. The last clearly identified TAG to elute was 9:0/9:0/9:0 which gave the upper mass limit ( $m/z$  512) for this GC-MS analysis.

In addition to fatty acids, GC-MS analysis of the saponified samples showed at least 35 1-*O*-alkylglycerol ethers as their TMS derivatives, which were found via their  $m/z$  205 ion as previously described [3] (for details, see ESM). The major components in samples from both sexes were the C13:0–18:0 alkyl glycerols, with C14:0 and 16:0 compounds being the most abundant.

The LC-MS data indicated that hydroxy fatty acids were present, although they had not been found amongst the TMS derivatised fatty acids and alcohols. A search was therefore made for hydroxy fatty acids, using FAME plus TMS derivatisation. There was good evidence for a C18:1 and C18:2 hydroxy TMS fatty acid methyl esters (see ESM for details). Although there was evidence of other hydroxy fatty acids, this was more ambiguous and is not reported here.

### LC-MS Analyses

Analysis of the total lipid extracts by LC-MS gave complex chromatograms of unresolved peaks (Fig. 1a). The mass spectra were averaged over the region where the lipids eluted (about 1.5–12 min; Fig. 1b). The cone voltage was optimised at 45 V to produce as principal ions the ammoniated lipid molecules ( $[M + NH_4]^+$ ), regardless of the mass of the lipid. As expected [12], higher cone voltages produced more in-source fragmentation of the short-chain lipids (TAG <28:0), while lower voltages resulted in low ionisation efficiencies for the longer-chain compounds. Figure 1b shows that the secretions contained lipids of a wide range of masses. Similar patterns were observed with samples from other possums, of both sexes. Using calculations based on the assumption that even-mass ions corresponded to the  $[M + NH_4]^+$  ions of TAG, the total numbers of acyl carbons and double bonds (Cn:x) were calculated

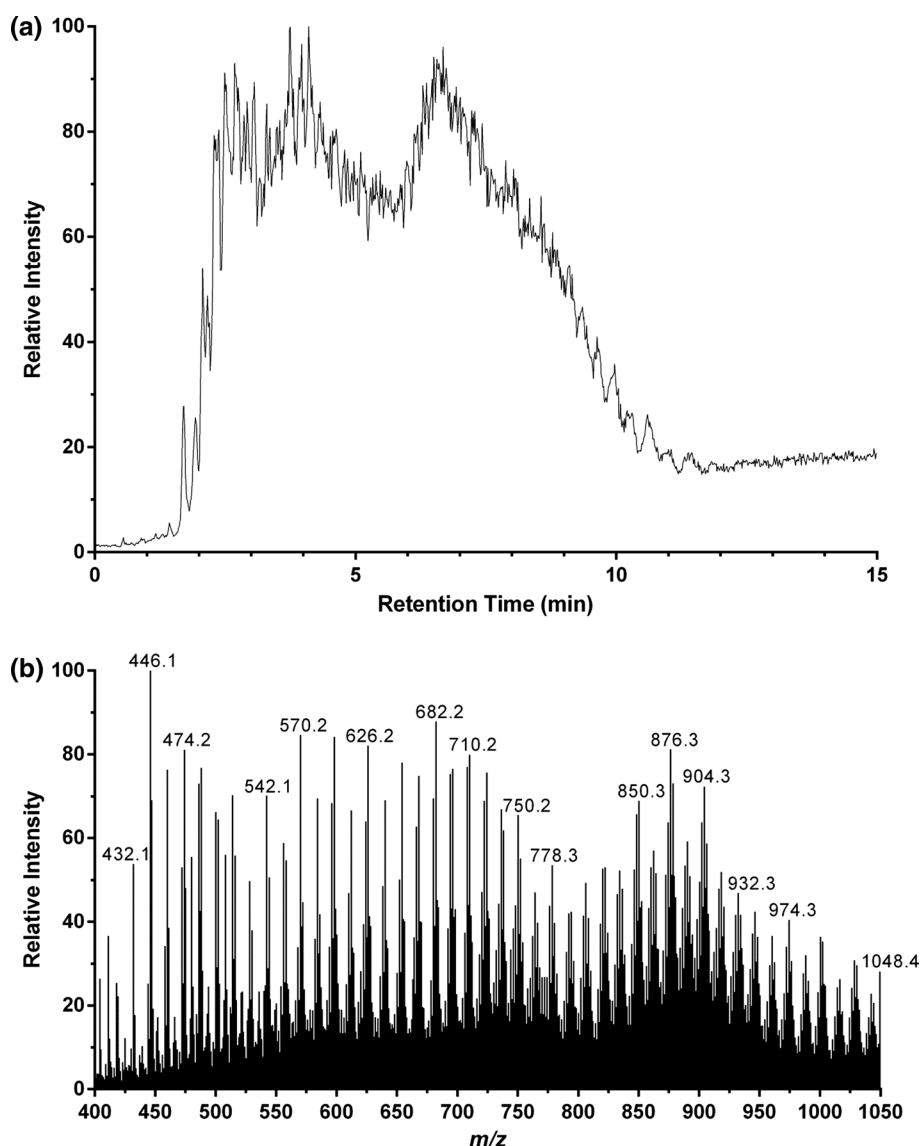
for selected ions. The short-chain TAG, from  $m/z$  404 (TAG 18:0) to about  $m/z$  696 (TAG 39:1), were followed continuously by longer-chain TAG to at least  $m/z$  1048 (TAG 64:0). As the mass and therefore chain length increased, so did the number of peaks. Many of the higher mass major ions indicated unsaturation, e.g.  $m/z$  874 (TAG 52:3),  $m/z$  878 (TAG 52:1),  $m/z$  904 (TAG 54:2),  $m/z$  1000 (TAG 61:3) and  $m/z$  1028 (TAG 63:3).

In order to investigate the individual lipids underlying this complex mixture, selected ion chromatograms were plotted. A number of these are shown in Fig. 2, in which the complexity of the chromatograms increased with mass from  $m/z$  446 to 928. With increasing mass the peaks broadened, indicating that there were more isomeric forms of the long-chain TAG coeluting within the same peak. This was as expected due to the greater possible number of acyl combinations in each high-mass TAG, and the greater number of branched isomers found in the long-chain fatty acids, as found previously [3] and confirmed in this study. However, it was also evident that the chromatograms showed multiple resolved peaks. Examination of the mass spectra enabled some of the peaks to be excluded as isotope peaks of lower masses, as indicated in Fig. 2. After this, it appeared that there were still up to three chromatographically distinct isobaric lipids present. These have been labelled EST, TAG and DAGE, anticipating our findings to come. The retention times (RT) of each of these peaks were plotted against  $m/z$ . Where there were multiple peak maxima, the largest was chosen. Peaks giving weak mass spectra (intensity  $<1.5e^5$ ) were ignored. Masses were labelled and organised by the calculated TAG level of unsaturation from Cn:0-6.

Figure 3 shows the plots of RT (min) versus  $m/z$  of ammonium adducts for masses equivalent to TAG with 0, 1, 2 and 4 double bonds. A similar pattern was found with 3 double bonds, while there were fewer compounds with 5 or 6 double bonds. It is evident that there were three groups of compounds, which eluted in the order EST, TAG and DAGE. Evidence for their structural assignments will now be presented.

Although Fig. 2 shows the chromatograms of single ions, the spectrum of each peak displayed all of the ions collected at that retention time. To select only the ions relevant to the compound of interest, MS-MS scans were used to display only the product ions of representative parent  $[M + NH_4]^+$  ions. LC-MS chromatograms of the product ions of  $m/z$  446 and 586 are shown in Fig. 4a. The retention times differed from those in Fig. 2 as they come from separate analyses. The products of  $m/z$  446 (TAG 21:0) showed a single broad peak, as for the parent ion in Fig. 2a. The product ion mass spectra were interpreted according to the known behaviour of acyl glycerols [10, 11]. Electro-spray mass spectrometry of TAG ammonium adduct ions

**Fig. 1** **a** LC–MS chromatogram for the paraloacal extract of a female possum showing the complex distribution of TAG, DAGE and other lipid species as ammoniated molecules. The TIC is the summed ion current chromatogram for the range  $m/z$  400–1050 acquired with a cone voltage of 45 V, optimised to display both short- and long-chain glycerides. **b** Average mass spectrum of the chromatogram in **a** for the region 1.5–12.0 min. Significant ions which could not be readily labelled were: 404.1 (26 %); 586.2 (42 %); 670.2 (40 %); 724.2 (76 %); 938.3 (33 %)



$[M + NH_4]^+$  results in the neutral loss of  $NH_3$  and  $RCOOH$  to give a (lyso) diacyl product ion. Dissociation of the diacyl product ions produces  $RCO^+$  and  $[RCO + 74]^+$  ions, and their dehydrated forms (less 18 Da).

The mass spectrum of  $m/z$  446 is shown in Fig. 4b (upper panel), and the ions found and their interpretation are as follows. The ions were:  $m/z$  299 (lyso 14:0, formed after neutral loss of fatty acid 7:0, 130 Da);  $m/z$  271 (lyso 12:0, after loss of FA 9:0); and  $[RCO - 18]^+$  ions at  $m/z$  95 (fatty acyl 7:0), 109 (acyl 8:0), and 123 (acyl 9:0). Additional ions were found at  $m/z$  285 and 313, indicating lyso 13:0 (e.g. 6:0/7:0) and 15:0 (e.g. 7:0/8:0). This mass spectrum was consistent with the structure being predominantly TAG 7:0/7:0/7:0 with some evidence of 6:0/7:0/8:0 and 6:0/6:0/9:0. Note that this structural notation is only used to list the FA present, as their *sn* positions are unknown. The broad peak could be due to the differing chromatographic

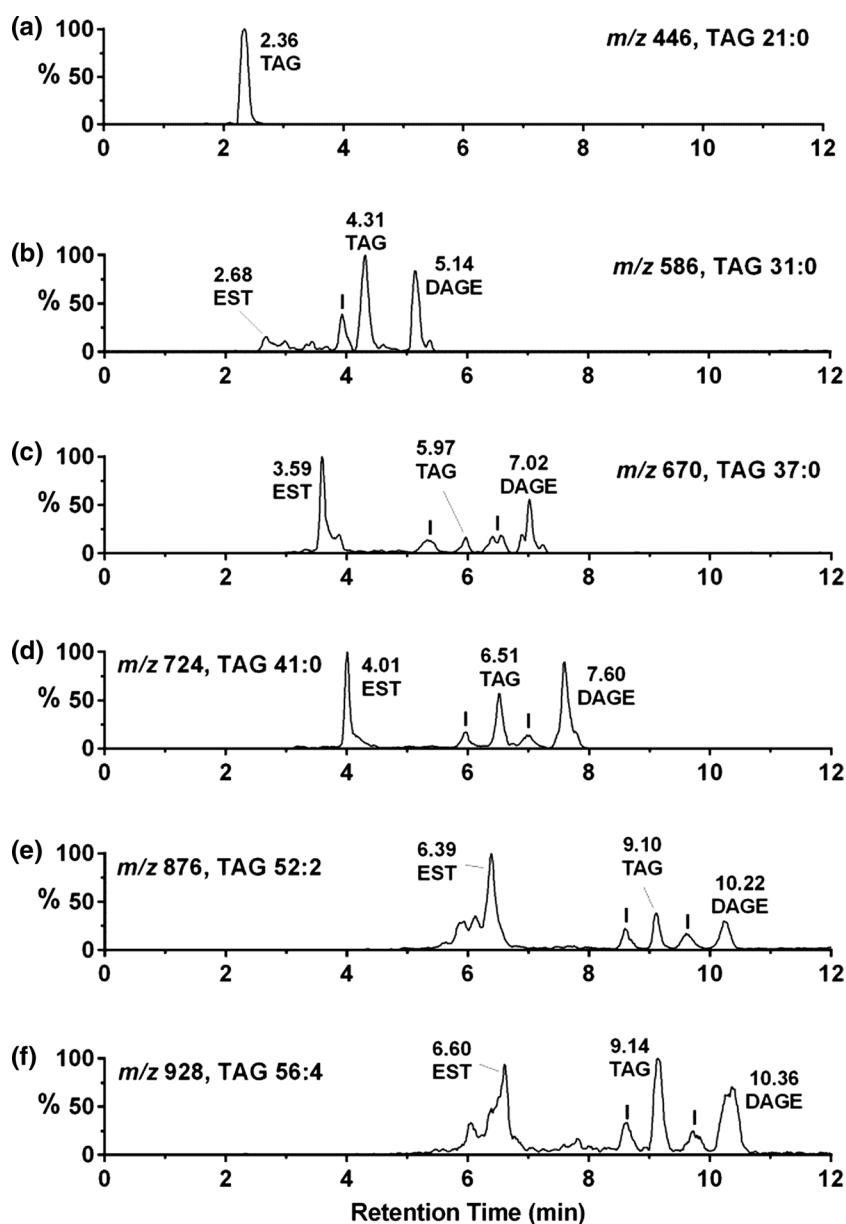
mobilities of the isomers of FA 7:0 (iso-, anteiso- and *n*-), as well as the contribution of other acids (6:0, 8:0 and 9:0) and their isomers.

The RT of five standard symmetrical TAG of *n*-acids (8:0, 10:0, 12:0, 14:0, 16:0) were plotted against mass which gave a good fit to a third order polynomial. Using this regression, and interpolating values for other saturated TAG, showed that the major components of possum lipid TAG eluted before the TAG of *n*-acids, indicating that they mainly comprised branched acids. This is consistent with the findings from GC–MS analyses of saponified samples in which iso- and anteiso-FA from C7:0–C9:0 were far more abundant than the *n*-isomers.

Similarly the chromatogram of product ions of  $m/z$  586 is shown in Fig. 4a (lower panel). Only the major peaks from the full scan ion chromatogram in Fig. 2 are shown, and the EST peak in Fig. 2b was too weak. Examination of



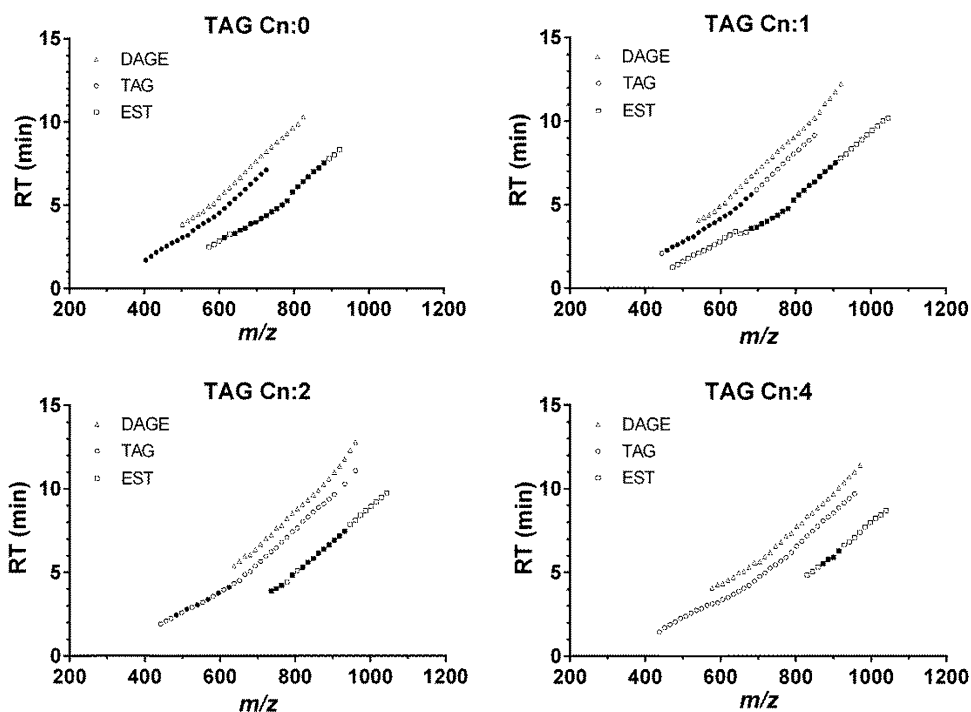
**Fig. 2** Selected ion chromatograms of some of the ammoniated molecules in Fig. 1. Isotope peaks are labelled I



the mass spectra in Fig. 2b showed that the peak eluting just before the TAG was principally due to an isotope peak of  $m/z$  584, and this was ignored where it appeared in Fig. 4b (at 4.53 min). The spectrum of the peak at 5.00 min. Figure 4b, (middle panel) showed neutral losses of every saturated fatty acid from 7:0 (NL 130 yielded  $m/z$  439) to 17:0 (NL 270 yielded  $m/z$  299). There were also  $[RCO - 18]^+$  ions from saturated FA 6:0 ( $m/z$  81), 7:0 ( $m/z$  95), 8:0 ( $m/z$  109), 9:0 ( $m/z$  123), 10:0 ( $m/z$  137) and 11:0 (151), as well as  $[RCO + 74]^+$  for 7:0 ( $m/z$  187). Thus the peak was TAG 31:0 from many combinations of acids, especially 7:0/7:0/17:0, 7:0/8:0/16:0 and 7:0/9:0/15:0. These isomers eluted close together as they have the same effective carbon number [13].

The next  $m/z$  586 peak (at 5.98 min in Fig. 4a, lower panel) had the same nominal mass as TAG 31:0 but eluted 1 min later, indicating that it was significantly less polar. This was expected for DAGE which have one more carbon and one less oxygen than the isobaric TAG. DAGE are also resolved from TAG by normal phase LC, where they elute earlier [14]. The mass spectrum of this peak (Fig. 4b, lowest panel) showed neutral losses of FA 7:0 and 9:0, and the  $[RCO - 18]^+$  ions of these acids at  $m/z$  95 and 123. The ion at  $m/z$  327 indicated a loss of 242 Da, equivalent to either a 15:0 acid or a 16:0 alcohol. As GC–MS analysis had found that 16:0 alkyl glycerol was the most abundant glycerol ether, and loss of ROH is an important loss from glycerol ethers [15], the peak was identified as predominantly

**Fig. 3** Plots of RT (min) versus ammoniated molecule  $m/z$  for compounds in Fig. 1. Open triangles DAGE, open circles TAG, open squares EST. Data are grouped according to the level of unsaturation of TAG (and DAGE). EST lipids have one more double bond. The filled symbols indicate compounds which were parents of  $m/z$  299, indicative of the presence of two C7:0 FA in the vast majority of cases



DAGE 32:0, 7:0/9:0/e16:0. Similarly, other isobaric pairs of TAG and DAGE were confirmed from their mass spectra, and four are labelled in Fig. 2c–f.

Figures 2 and 3 show that the unknown lipids (EST) eluted well before TAG and DAGE of the same nominal mass, and were therefore more polar. The magnitude of this difference was assessed by comparing the shift in RT from EST to TAG to DAGE, using the data in Fig. 3 for masses where all three lipids were present. On average, the difference in RT between EST and TAG was 2.1 times that from TAG to DAGE (SD 0.5,  $n = 56$ ), indicating a commensurately larger difference in polarity and structure.

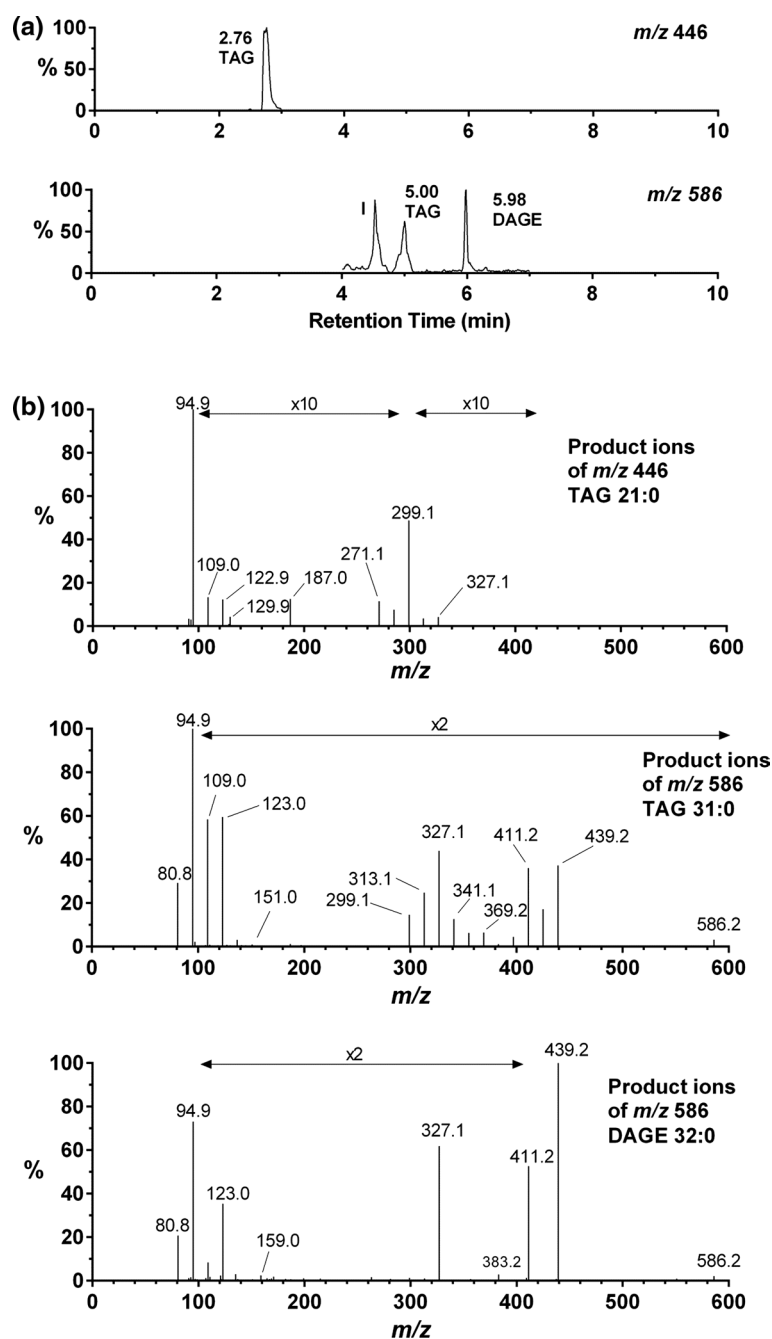
The unknown lipids had complex mass spectra, which were difficult to interpret particularly given the coelution of numerous isomers. However, examination of product ion spectra from a number of their peaks showed a prominent lyso ion at  $m/z$  299 (14:0). MS–MS analysis showed that, after generation of  $m/z$  299 by ‘in source’ fragmentation, the only significant product ion derived from this was  $m/z$  95, corresponding to the FA 7:0 acyl ion  $[\text{RCO} - 18]^+$ . Thus this  $m/z$  299 lyso ion had the same structure for all compounds (except for possible regioisomerism) indicating that it was 7:0/7:0. Parents of this ion have only one remaining substituent on glycerol, thus simplifying their identification. Therefore, analysis of the unknown lipids focused on the parents of  $m/z$  299, which are shown in Fig. 3 with half-filled symbols.

The most abundant ion in the average mass spectrum for parents of  $m/z$  299 was at  $m/z$  876. The plot of  $m/z$  876 (52:2 when present as a TAG) from the full scan

chromatogram showed three distinct peak groupings, excluding those attributable to isotope peaks (Fig. 2e). The LC–MS–MS product ion chromatogram of  $m/z$  876 showed three peaks, at RT 7.47, 9.90 and 10.67 min (Fig. 5a), and their mass spectra are shown in Fig. 5b. Each peak exhibited the  $[\text{MH}]^+$  ( $m/z$  859) ion from loss of  $\text{NH}_3$  from the ammonium adduct, however the other EST ions were quite different from those for TAG and DAGE. The TAG spectrum (Fig. 5b, upper panel) predominantly showed losses of acids 14:0, 16:0, 18:1 and 20:1, with some corresponding acyl-related ions, indicating that major components of this peak were 14:0/18:1/20:1 and 16:0/18:1/18:1 (TAG 52:2). The DAGE spectrum (Fig. 5b, middle panel) showed some of the same ions, especially  $m/z$  603 corresponding to loss of 17:0 alcohol and/or 16:0 acid, and  $m/z$  577 corresponding to the loss of 19:1 alcohol and/or 18:1 acid. Since the GC–MS analysis showed 17:0 alkyl glycerol (see ESM) to be much more abundant than 19:1 alkyl glycerol, the more likely DAGE structure was 17:0e/18:1/18:1 (53:2).

The major ion in the EST spectrum was  $m/z$  299 (Fig. 5b, lowest panel) which was absent from both TAG and DAGE spectra. Since  $m/z$  299 had been shown to be due almost entirely to the 7:0/7:0 lyso ion, the unknown lipid seemed to be a TAG with acyl groups 7:0/7:0/38:2. GC–MS analysis had, however, found no fatty acids greater than 24:0 (see ESM). Also, the other most significant fragment ions, such as  $m/z$  447, 449, 475 and 477, could not be interpreted from this TAG structure. Furthermore, a TAG of this structure would be expected to elute near its isobaric 52:2 TAG, whereas this lipid eluted 2.4 min earlier. These

**Fig. 4** **a** LC–MS chromatograms of product ions of ammonium adduct ions  $m/z$  446 (TAG 21:0) and  $m/z$  586 (TAG 31:0, DAGE 32:0). The isotope peak (I) was formed from  $m/z$  584, as found from the full scan chromatogram. **b** Mass spectra of product ion peaks of product ion peaks in **a**, showing TAG and DAGE compounds derived from the parent molecular ions  $m/z$  446 and  $m/z$  586



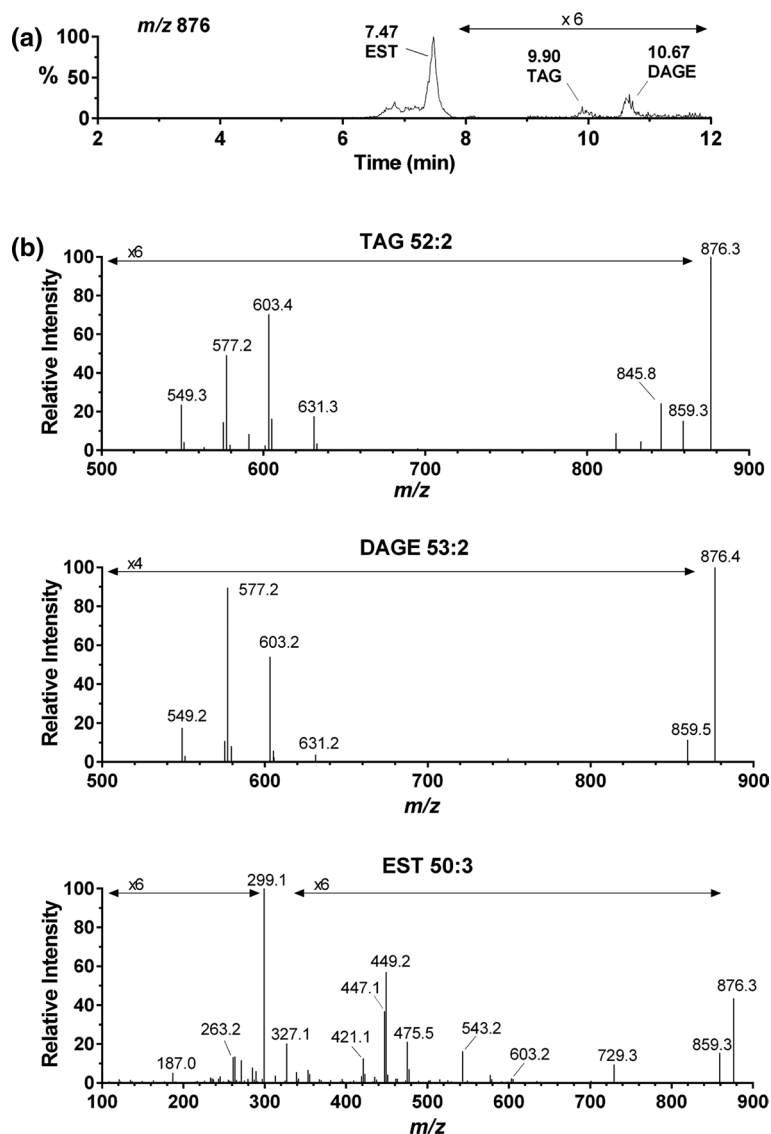
observations pointed to a significantly different structure for the unknown lipid.

A pseudo-MS<sup>3</sup> experiment was performed in which a higher cone voltage was used to induce in-source production of the diagnostic product ions so that their structure could be examined further by MS–MS. LC–MS–MS analysis of product ions of  $m/z$  449, a major ion in the EST spectrum, showed peaks at both early (3.81 min) and later (6.28 min) times, indicating that this ion was formed from both TAG and EST lipids. The peak at 3.81 min corresponded with the ammoniated TAG 32:2 ion  $m/z$  596,

which was identified at this time on full scan and gave lyso ions at  $m/z$  299 (14:0) and  $m/z$  449 (25:2). The product ions of  $m/z$  449 (Fig. 6a) showed acyl ions for FA 7:0 ( $m/z$  95, 113, 187) and FA 18:2 ( $m/z$  245, 263, 319). This TAG was identified as 7:0/7:0/18:2, and the  $m/z$  449 ion as lyso 25:2 (7:0/18:2). The later peak, at 6.28 min, was also examined as this corresponded to the unknown ammoniated acylglycerol EST  $m/z$  876 in the full scan chromatogram, and here the products of  $m/z$  449 showed the same ions (Fig. 6b) indicating that this was also a 25:2 lyso ion, 7:0/18:2.



**Fig. 5** **a** LC–MS chromatograms of product ions of ammonium adduct ions  $m/z$  876, showing peaks identified as EST, TAG and DAGE lipids. **b** Mass spectra of peaks in **a** showing characteristic ions for three types of lipid: TAG and DAGE and EST

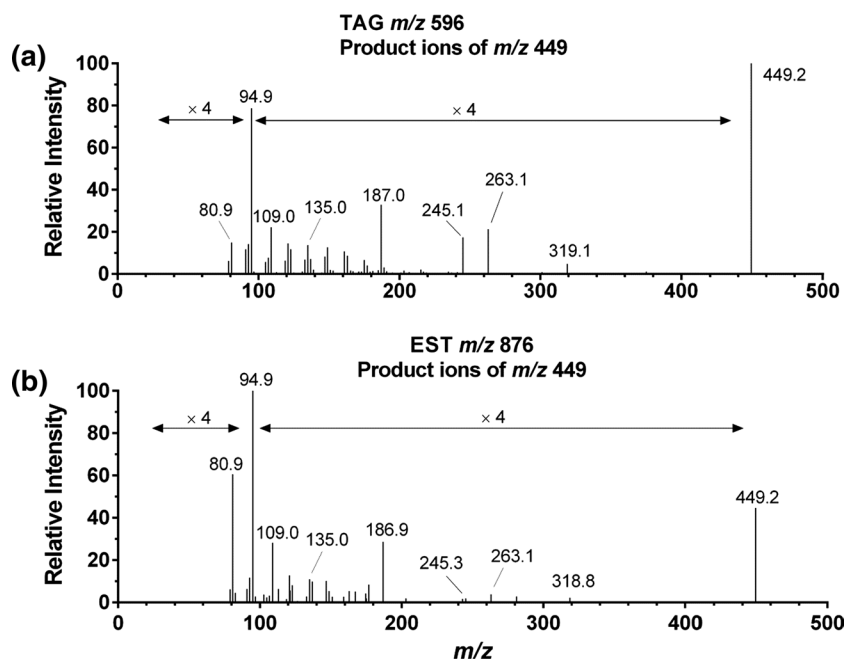


It is proposed that the EST 25:2 product ion was formed from a precursor TAG 7:0/7:0/18:2  $[M + H]^+$  ion, which in turn was formed from a TAG-estolide  $[M + NH_4]^+$  parent ion in which a fourth acyl group (FA 18:2) had been joined by an estolide linkage to an 18:1 hydroxy acyl group which was itself attached to the glycerol backbone. The neutral loss of the 18:2 RCOOH plus  $NH_3$  from EST  $m/z$  876 left an ion equivalent to the protonated TAG 32:2 ( $m/z$  579). This process entailed the loss of  $H_2O$  from the 18:1 hydroxy acyl group, which became an 18:2 acyl group. The loss of  $H_2O$  accompanies all neutral losses of fatty acids from TAG, or fatty alcohols from DAGE [10, 11, 15]. In this case, the parent TAG-estolide structure was 7:0/7:0/h18:1–18:2.

Table 1 shows that the estolide hypothesis accounts for all the significant ions formed (Fig. 5b) as products of several isomers of EST 50:3, and Fig. 7 shows the general

fragmentation of TAG-estolides schematically. Neutral loss of a fatty acid plus  $NH_3$  from the ammoniated parent gave three types of product ion. Cleavage of the estolide bond gave a  $[TAG + H]^+$  product ion. Loss of the entire estolide acyl group as  $R_4COOR_3COOH$  gave the usual type of TAG-lyso ions. In this case, these were all short-chain diacylglycerols, including the abundant ions of 7:0/7:0 ( $m/z$  299, 100 %) and 7:0/9:0 ( $m/z$  327, 20 %). TAG-lyso ions were also formed from the  $[TAG + H]^+$  product ion, giving a medium-chain acyl group if the residual estolide FA was retained (e.g. 7:0/18:2  $m/z$  449, 10 %). Loss of a non-estolide FA from the glycerol backbone of the parent TAG-estolide gave a lyso-estolide product ion. In the example of EST 7:0/7:0/h18:1–18:2, NL of 7:0 gave the lyso-estolide ion 7:0/h18:1–18:2 (43:3,  $m/z$  729, 1.5 %). This ion is analogous to TAG-lyso ions except that the relationship between mass and acyl Cn:x is different (TAG-lyso  $m/z$  729 is 45:2).

**Fig. 6** Mass spectra of product ions of  $m/z$  449 formed from TAG 32:2  $m/z$  596 (RT 3.81 min) and EST 50:3  $m/z$  876 (RT 6.28 min) ammonium adduct ions



Further fragmentation of the TAG- or estolide-lyso ions produced ions characteristic of the remaining acyl groups:  $\text{RCO}^+$ ,  $\text{RCOORCO}^+$ ,  $[\text{RCO} + 74]^+$ ,  $[\text{RCOORCO} + 74]^+$  and their dehydrated forms, as described for TAG [10]. In this example, acyl-related ions were found for FA 7:0 ( $m/z$  187), FA 18:2 ( $m/z$  263, 245) and FA-estolide 36:3 ( $m/z$  543, 525 and 599). Other neutral losses and lyso and acyl ions indicated the presence of 14 more FAs from 9:1 to 20:4 (Table 1). This showed that there were a number of isobaric compounds contributing to the mass spectrum. All had two short chain acyl groups (mostly 7:0 and 9:0) and one longer chain estolide group (mostly 36:3 and 34:3, comprised of combinations of 16:1, 16:2, 18:1 and 18:2 fatty acids). Masses equivalent to estolide acyl groups (33:2, 33:3, 34:2, 34:3, 35:3, 36:3) were also lost, and ions corresponding to the expected acyl-estolides were observed. Hydroxy fatty acids (18:1 and 18:2) were detected in the FAME analysis of saponified samples (see GC–MS Analyses and ESM), lending further support to the estolide hypothesis.

### Accurate Mass Measurements by LC–MS

Subsequent accurate mass measurements of the lipids (as  $[\text{M} + \text{Na}]^+$  ions) confirmed the formulae for these three distinct lipid compound series: O8 EST, O6 TAG and O5 DAGE. Figure 8 shows the high resolution LC–MS chromatogram for the sodium adduct ion of nominal mass  $m/z$  729 (which corresponds to the ammonium adduct ion  $m/z$  724 in the low resolution chromatogram in Fig. 2d). The three lipids were clearly separated in time and mass, with accurate values of  $m/z$  729.5279 ( $\text{C}_{42}\text{H}_{74}\text{O}_8\text{Na}$ , 0.42 ppm error; TAG-estolide 39:2),  $m/z$  729.6009 ( $\text{C}_{44}\text{H}_{82}\text{O}_6\text{Na}$ ,

0.74 ppm error; TAG 41:1) and  $m/z$  729.6370 ( $\text{C}_{45}\text{H}_{86}\text{O}_5\text{Na}$ , 0.35 ppm error; DAGE 42:1). EST 50:3 ( $m/z$  876 as the ammonium adduct,  $m/z$  881 as the sodium adduct) was measured as 881.6847 giving the formula  $\text{C}_{53}\text{H}_{94}\text{O}_8\text{Na}$  (0.74 ppm error). The isobaric TAG 52:2 had a mass of 881.7576 giving the formula  $\text{C}_{55}\text{H}_{102}\text{O}_6\text{Na}$  (1.27 ppm error). The accurate mass measurements showed that there were about 150 different molecular formulae for EST lipids. This agreed with the count of 148 EST lipids from the RT *versus*  $m/z$  data in Fig. 3 (all EST from  $\text{C}_n:0$ -5).

### Levels of Unsaturation Amongst Longer-Chain Lipids

Initially all compounds had been labelled and grouped by their carbon number and level of unsaturation as if they had been TAG. However, the mass of a  $\text{C}_n:x$  TAG corresponds to a  $\text{C}(n+1):x$  DAGE and a  $\text{C}(n-2):(x+1)$  EST. Thus, the data on DAGE and EST in Fig. 3 can be corrected for  $\text{C}_n:x$ . Since saturated EST values were not plotted, this was examined separately and the compounds found to range from EST 24:0 to 39:0.

To show the range of compounds and their levels of unsaturation in the longer-chain members of the three lipid groups, plots were made of RT *versus* mass for each carbon number from  $\text{C}_n:0$  to  $\text{C}_n:x$  in decrements of 2 mass units until the unsaturated series was exhausted (Fig. 9). Data were obtained from LC–MS ion chromatograms from a full scan run, as in Fig. 3. RT were recorded for the largest peak in a group, or the mid-point of a cluster of peaks. The mass spectra were examined and peaks were excluded if they did not clearly show the selected ion and its expected isotopes. Only the range  $m/z$  780–902 was plotted, as lower masses

**Table 1** Ions found from the LC–MS–MS analysis of the  $[M + NH_4]^+$  ion of TAG-estolide 50:3 (*m/z* 876), including structural interpretation (Fig. 5b) *m/z*

Ion found (Fig. 5b) <i>m/z</i>	%BP	Product ion type	Acyl groups remaining <sup>a</sup>	NL (Da)	Acyl Cn:x for acid(s) lost		Confirmatory acyl ions found ( <i>m/z</i> ) <sup>b</sup>				Parent TAG-EST <sup>c</sup> (other isomers may be possible)	
					FA	FA-EST	RCO <sup>+</sup>	[RCO – H <sub>2</sub> O] <sup>+</sup>	[RCO + 74] <sup>+</sup>	[RCO + 74 – H <sub>2</sub> O] <sup>+</sup>		
859	2.5	MH <sup>+</sup>	50:3-estolide	17 <sup>d</sup>	–	–	–	–	–	–	50:3-estolide	
729	1.5	Lyso-estolides from NL of a glyceryl FA	7:0/36:3-estolide	130	7:0	–	ns	187	–	–	7:0/7:0/36:3-estolide	
703	0.1		7:0/34:2-estolide	156	9:1	–	121	–	–	–	7:0/9:1/34:2-estolide	
701	0.2		7:0/34:3-estolide	158	9:0	–	123	215	–	–	7:0/9:0/34:3-estolide	
605	0.2	[TAG + H] <sup>+</sup> from NL of the terminal estolide FA	7:0/7:0/20:3	254	16:1	237	–	311	–	–	7:0/7:0/h20:2–16:1	
603	0.2		7:0/7:0/20:4	256	16:0	–	–	313	–	–	7:0/7:0/h20:3–16:0	
591	0.1		7:0/7:0/19:3	268	17:1	–	233	325	307	–	7:0/7:0/h19:2–17:1	
579	0.2		7:0/7:0/18:2	280	18:2	263	245	–	–	–	7:0/7:0/h18:1–18:2	
577	0.5		7:0/7:0/18:3	282	18:1	265	–	339	–	–	7:0/7:0/h18:2–18:1	
549	0.2		7:0/7:0/16:3	310	20:1	–	275	367	–	–	7:0/7:0/h16:2–20:1	
477	1.1	Lyso ions from NL of a FA from the [TAG + H] <sup>+</sup> product ion	9:0/18:2	382	7:0 + 16:2	235	217	–	–	–	7:0/9:0/h18:1–16:2	
475	3.5		7:0/20:3	384	7:0 + 16:1	237	–	311	–	–	7:0/7:0/h 20:2–16:1	
449	9.5		7:0/18:2	410	7:0 + 18:2	263	245	–	–	–	7:0/7:0/h18:1–18:2	
447	6.2		7:0/18:3	412	7:0 + 18:1	265	–	339	–	–	7:0/7:0/h18:2–18:1	
421	2.1		7:0/16:2	438	9:0 + 18:2	263	245	–	–	–	7:0/9:0/h16:1–18:2	
419	0.6		7:0/16:3	440	9:0 + 18:1	265	–	339	–	–	7:0/9:0/h16:2–18:1	
341	0.5	Lyso ions from NL of the estolide FA	8:0/9:0	518	–	501	–	–	–	–	8:0/9:0/33:3-estolide	
339	0.7		8:0/9:1	520	–	503	–	577	559	–	8:0/9:1/33:2-estolide	
327	19.9		7:0/9:0	532	–	515	–	–	–	–	7:0/9:0/34:3-estolide	
325	1.0		7:0/9:1	534	–	–	591	591	–	–	7:0/9:1/34:2-estolide	
313	3.8		7:0/8:0	546	–	529	–	603	–	–	7:0/8:0/35:3-estolide	
299	100		7:0/7:0	560	–	543	525	–	599	–	7:0/7:0/36:3-estolide	
Other FA lost from [TAG + H] <sup>+</sup> ions (or isomers) above												
			<i>m/z</i> 579 → 327	252	16:2	235	217	–	291	–		
			<i>m/z</i> 579 → 299	250	16:3	233	215	307	289	–		
			<i>m/z</i> 549 → 299	278	18:3	261	243	–	–	–		
			<i>m/z</i> 577 → 299	276	18:4	259	–	–	–	–		
			<i>m/z</i> 591 → 299	292	19:3	275	–	–	–	–		
			<i>m/z</i> 605 → 299	306	20:3	289	271	–	–	–		
			<i>m/z</i> 603 → 299	304	20:4	287	269	–	–	–		

NL from the ammoniated molecule comprised the elements of FA plus NH<sub>3</sub> (or the ammoniated salt), as shown in Fig. 7

ns not scanned, – not found or not applicable

<sup>a</sup> Or isomers, for example 7:0/7:0/20:4 and 7:0/9:0/18:4

<sup>b</sup> Where two acids have been lost, the acyl ions are given for the second acid

<sup>c</sup> Note that loss of the terminal estolide FA results in dehydration of the remaining estolide FA

<sup>d</sup> Loss of NH<sub>3</sub>

**Fig. 7** Scheme showing the formation of product ions from the dissociation of TAG-estolide  $[M + \text{NH}_4]^+$  ions, based on the example of  $m/z$  876 (EST 50:3). As the *sn* positions on glycerol are not known, and  $R_1$  and  $R_2$  are equivalent in this example, not all isomers are shown. Acyl ions no longer linked to the glycerol backbone ( $\text{RCO}^+$  and  $\text{RCO}^+ - \text{H}_2\text{O}$ ) are not included.  $\text{R}'_3\text{CO}$  denotes the dehydrated form of the acyl group of the hydroxy fatty acid  $\text{R}_3\text{COOH}$ . Details of all ions are given in Table 1

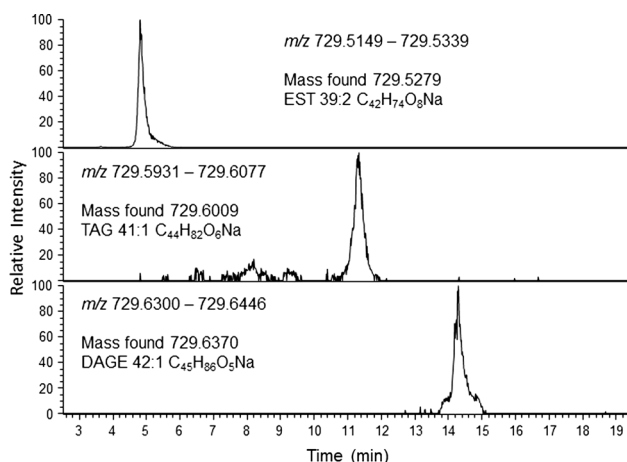
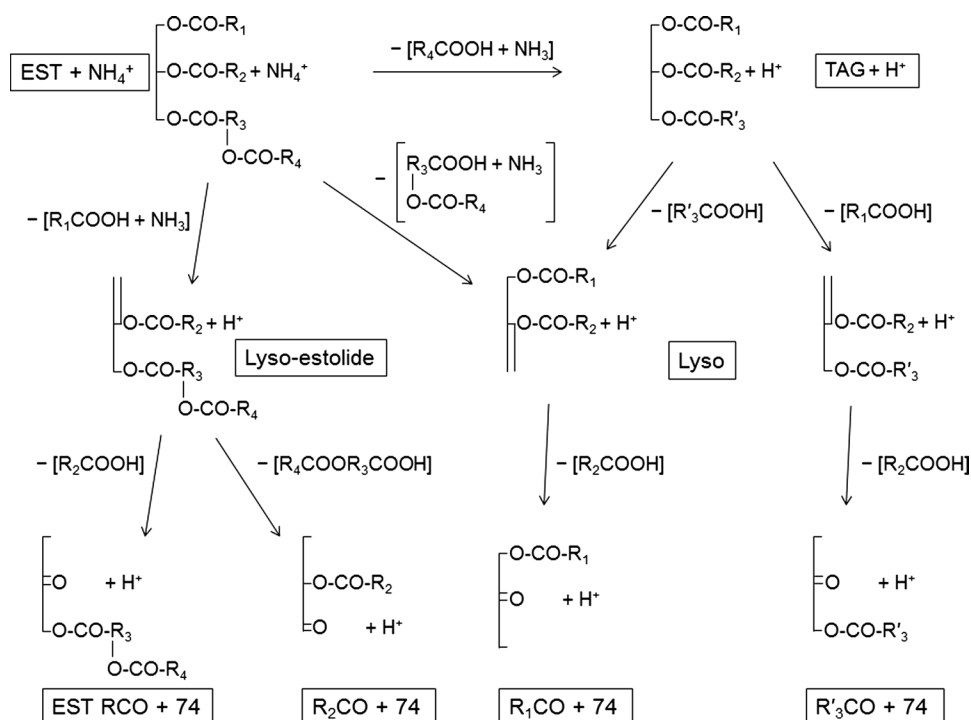


**Fig. 8** LC-MS chromatograms of accurate masses of EST, TAG and DAGE of nominal mass  $m/z$  729 (sodium adducts), equivalent to  $m/z$  724 ( $\text{NH}_4^+$  adducts)

had fewer double bonds and larger masses gave more complex chromatograms whose peaks were difficult to assign.

In Fig. 9 the vertical lines link isobaric compounds. Regression lines are shown for the  $\text{C}_n:1$  compounds, and can be fitted to each level of unsaturation. Each lipid type showed several series of points of different carbon number, with RT decreasing with  $m/z$ , although not all possible masses were found. For example, DAGE  $m/z$  892 (54:1) commenced a regression of increasing unsaturation to  $m/z$  880 which was assigned to DAGE 54:7 and not the isobaric 53:0 because of the RT (8.03 min). There was no DAGE

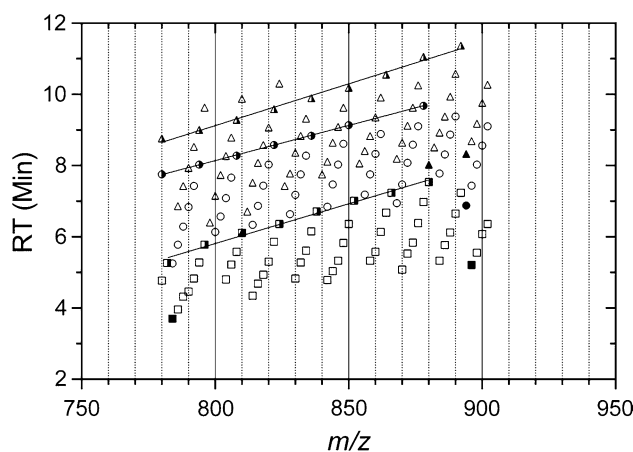


**Fig. 9** Levels of unsaturation in three classes of lipids, displayed by plotting RT (min) against  $m/z$  (range 780–902). Open triangle DAGE, open circle TAG, open square EST. Not all levels of unsaturation were found, and to clarify the data compounds with one double bond ( $\text{C}_n:1$ ) are indicated by half-fill in the symbols and a linear regression line fitted.  $\text{C}_n:7$  compounds are shown with full-fill

53:0, and the next regression started with  $m/z$  878, DAGE 53:1 (11.05 min). In this manner, DAGE compounds were plotted from C47–55, showing only three saturated compounds (47:0–49:0) and all levels of unsaturation mostly up to six or seven double bonds. There were no saturated TAG in this range (C46–54), and unsaturation mostly ended with five double bonds, although there was one compound with seven (54:7). There were no saturated estolides, each set from C43–50 starting with one double bond and ending

with 5–7 double bonds. The chromatogram of  $m/z$  810 gave one peak at 9.88 min (DAGE 48:0) and a broad peak with multiple maxima around 6.11 min. This was interpreted as a mixture of compounds, including DAGE 49:7 and EST 45:1, and all these points are plotted in Fig. 9.

The approach shown in Fig. 9 seems to be a useful way of interrogating complex data to reveal the range of compounds and their levels of unsaturation. In most cases, additional LC–MS experiments would be required for more definitive individual assignments. Moreover, as only the most significant peaks are investigated, the plot underestimates the number of compounds present. However, it does provide an overview of significant compounds present in an otherwise obscure mixture.

### Body Fat

LC–MS showed that renal fat predominantly comprised TAG of 50:1-3, 52:1-5 and 54:2-7, and abdominal fat was similar. The smallest significant TAG was at  $m/z$  820 (48:2) and the largest,  $m/z$  924 (56:6). GC–MS analysis of FAME revealed that the fatty acids were also the same in both samples, and comprised (in descending order) FA 18:1 (c.39 %), 16:0 (c. 23 %), 18:2 (c. 16 %), 18:3w3 (c. 10 %), 18:0 (c. 8 %) and 14:0 (c. 2 %) with traces of two 16:1 isomers and 17:1. There were no short chain fatty acids and almost none were odd-numbered. Thus the body fat showed the usual composition for mammals.

### Discussion

Although there have been several reports of triacylglycerol-estolides in plants [5–7], this is the first report of their occurrence in animals. Initially the analysis was difficult because of the complexity of the sample, with LC–MS showing a large number of acylglycerols of many fatty acids eluting together as unresolved peaks. However, when single ion chromatograms were plotted, three distinct groups of lipids became apparent. MS–MS analyses of selected  $[M + NH_4]^+$  ions enabled TAG to be identified from their characteristic NL of FA, and the formation of lyso ions and acyl-related ions. DAGE gave the same ions and were distinguished from TAG by their later elution time supported by the finding of glycerol ethers by GC–MS. The isobaric TAG-estolides were the earliest eluting group of lipids, and showed similar neutral losses and product ions to the TAG compounds, as well as other ions which were difficult to identify. The finding that many TAG-estolides and TAG shared the 7:0/7:0 substitution, and the realisation that the third substituent had a much greater mass than could be accounted for by the FA found by GC–MS, enabled it to be identified as a FA-estolide. This structure

provided the basis for interpretation of distinctive TAG-estolide product ions, particularly NL of RCOOH yielding  $[TAG + H]^+$ , lyso-estolide ions and acyl-estolide related ions were reported.

Published reports of TAG-estolides from plants all used sodium or lithium adduct ions, and found ions from NL of one or two RCOOH or the FA-estolide RCOORCOOH [5–7]. The estolide link was cleaved when formed from secondary alcohols ricinoleic acid (12OH C18:1) [5] and lesquerolic acid (14OH C20:1) [7] but not with the primary alcohol kamlolenic acid (18OH C18:3) [6]. There was an abundant ion for  $[RCOORCOOH + Na/Li]^+$  and some  $[RCOOH + Na/Li]^+$  but no acyl degradation ions.

Other possible structures were considered for the unknown lipids, but none explained the data as comprehensively as the estolide structure. Alkyl triacylglycerol glycerols have also been reported on a glycerylglycerol backbone [16]; however, the GC-MS analyses of saponified samples found only glycerol and no evidence of glycerylglycerol. Also, the fragmentation did not support this structure, especially the formation of the estolide acyl-related groups and the  $[TAG + H]^+$  ion from loss of the terminal estolide acid. Hydroxyalkylglycerols have also been reported [17, 18], but these have 7 oxygens whereas the TAG-estolides had eight. The identification of TAG-estolides was supported by the finding of hydroxy fatty acids after saponification.

Lipids, mostly fatty acids and alcohols and steroids and their esters, are a common finding amongst mammalian semiochemicals where they are usually considered to act as a vehicle to retard the release of the volatile compounds which act as chemical messengers (e.g. in the marking fluid of tigers and other large felids [19]). However, individual differences in lipid composition have suggested that they may also have a role in conspecific recognition (e.g. femoral gland secretions of iguanas [20]; subaxillary secretions of the fishing bat [21]). Glycerol monoethers are widespread in marine and terrestrial animals, where they occur as diacylglycerol ethers, many of which are biologically active [22]. The biological significance of the present finding of a complex mixture of three classes of lipids formed from many short- and medium-chain fatty acids, giving hundreds of different molecular species, is not known. Other body fat showed the usual mammalian profile, indicating that the paracloacal lipid mixture has evolved to suit a specific function. Moreover, its complexity suggests that it is not simply acting a vehicle for the many volatile chemicals which give the secretion its strong odour. Rather, this suggests that the lipids themselves contribute to the semiochemical messages between individuals, just as lipids are known to function as intercellular signalling molecules within individuals [23–25].

Paracloacal glands have been found in all marsupials studied, both in Australia and South America [1, 26].



These marsupials have been separated since the geological breakup of Gondwana 45 million years ago [27], and the conservation of paracloacal glands suggests a continued usefulness, which may however have diverged in the various modern species. In marsupials of both continents, the paracloacal glands show sexual dimorphism, evidence of endocrine control, a smell which humans find unpleasant, and a high lipid content [1, 26]. A comparative study of both the odiferous and lipid content of marsupial paracloacal glands may provide insights into their role(s), and evolutionary relationships since the phylogenetic tree of marsupials is now being well-elucidated [28].

In this study we have described methods which could be used to investigate other glycerol lipid mixtures for different classes of compounds, such as estolides and glycerol ethers. The availability of suitable analytical methods can reveal surprising complexity in lipids and lead to a fuller understanding of the biological role of different molecular species, as demonstrated by the discovery of monoalk(en) diacylglycerols in adiposomes [29].

**Acknowledgments** We thank Euan Thompson and Taryn Skinner (AgResearch Invermay, Mosgiel, New Zealand) for the capture and care of the possums and for dissection of the glands. We also thank Dr. Richard Wilson (Central Science Laboratory, University of Tasmania) for generating the accurate mass data. Funding for this study was provided by the Division of Pharmacy, School of Medicine, University of Tasmania. We are grateful to the anonymous referees for their comments which improved the manuscript.

## References

- McLean S (2014) Scent glands of the common brushtail possum (*Trichosurus vulpecula*). *N Z J Zool* 41:193–202
- Woolhouse AD, Weston RJ, Hamilton BH (1994) Analysis of secretions from scent-producing glands of brushtail possum (*Trichosurus vulpecula* Kerr). *J Chem Ecol* 20:239–253
- McLean S, Davies NW, Wiggins NL (2012) Scent chemicals of the brushtail possum, *Trichosurus vulpecula*. *J Chem Ecol* 38:1318–1339
- Zerkowski JA, Nunez A, Solaiman DKY (2008) Structured estolides: control of length and sequence. *J Am Oil Chem Soc* 85:277–284
- Lin JT, Arcinas A, Harden LR, Fagerquist CK (2006) Identification of (12-ricinoleoylricinoleoyl) diricinoleoylglycerol, an acylglycerol containing four acyl chains, in castor (*Ricinus communis* L.) oil by LC-ESI-MS. *J Agric Food Chem* 54:3498–3504
- Smith MA, Zhang HX, Forseille L, Purves RW (2013) Characterization of novel triacylglycerol estolides from the seed oil of *Mallotus philippensis* and *Trewia nudiflora*. *Lipids* 48:75–85
- Lin JT, Chen GQ (2013) Identification of tetraacylglycerols in lesquerella oil by electrospray ionisation mass spectrometry of the lithium adducts. *J Am Oil Chem Soc* 90:1831–1836
- McLeod BJ, Thompson EG, Crawford JL, Shackell GH (1997) Successful group housing of wild-caught brushtail possums (*Trichosurus vulpecula*). *Anim Welf* 6:67–76
- Murphy RC (1993) Triacylglycerols, diacylglycerols, and monoacylglycerols. *Mass spectrometry of lipids*. Plenum, New York
- McAnoy AM, Wu CC, Murphy RC (2005) Direct qualitative analysis of triacylglycerols by electrospray mass spectrometry using a linear ion trap. *J Am Soc Mass Spectrom* 16:1498–1509
- Murphy RC, James PF, McAnoy AM, Krank J, Duchoslav E, Barkley RM (2007) Detection of the abundance of diacylglycerol and triacylglycerol molecular species in cells using neutral loss mass spectrometry. *Anal Biochem* 366:59–70
- Hunt SM, Sheil MM, Belov M, Derrick PJ (1998) Probing the effects of cone potential in the electrospray ion source: consequences for the determination of molecular weight distributions of synthetic polymers. *Anal Chem* 70:1812–1822
- Buchgraber M, Ullberth F, Emons H, Anklam E (2004) Triacylglycerol profiling by using chromatographic techniques. *Eur J Lipid Sci Technol* 106:621–648
- Hutchins PM, Barkley RM, Murphy RC (2008) Separation of cellular nonpolar neutral lipids by normal-phase chromatography and analysis by electrospray ionisation mass spectrometry. *J Lipid Res* 49:804–813
- Hartvigsen K, Ravandi A, Bukhave K, Holmer G, Kuksis A (2001) Regiospecific analysis of neutral ether lipids by liquid chromatography/electrospray ionisation/single quadrupole mass spectrometry: validation with synthetic compounds. *J Mass Spectrom* 36:1116–1124
- Kasama K, Blank ML, Snyder F (1989) Identification of 1-alkyl-2-acyl-3-(2',3'-diacylglycerol)glycerols, a new type of lipid class, in Harderian gland tumors of mice. *J Biol Chem* 264:9453–9461
- Kasama K, Rainey WT, Snyder F (1973) Chemical identification and enzymatic-synthesis of a newly discovered lipid class—hydroxyalkylglycerols. *Arch Biochem Biophys* 154:648–658
- Blank ML, Snyder F, Kasama K (1972) Isolation and identification of an alkyldiacylglycerol containing isovaleric acid. *J Lipid Res* 13:390–395
- Burger BV, Viviers MZ, Bekker JPI, le Roux M, Fish N, Fourie WB, Weibchen G (2008) Chemical characterization of territorial marking fluid of male Bengal tiger, *Panthera tigris*. *J Chem Ecol* 34:659–671
- Alberts AC (1993) Chemical and behavioral studies of femoral gland secretions in Iguanid lizards. *Brain Behav Evol* 41:255–260
- Brooke AP, Decker DM (1996) Lipid compounds in secretions of fishing bat, *Noctilio leporinus* (Chiroptera: Noctilionidae). *J Chem Ecol* 22:1411–1428
- Magnusson CD, Haraldsson GG (2011) Ether lipids. *Chem Phys Lipids* 164:315–340
- Brown HA, Murphy RC (2009) Working towards an exegesis for lipids in biology. *Nat Chem Biol* 5:602–606
- Spite M, Serhan CN (2010) Novel lipid mediators promote resolution of acute inflammation impact of aspirin and statins. *Circ Res* 107:1170–1184
- O'Donnell VB, Murphy RC, Watson SP (2014) Platelet lipidomics: a modern day perspective on lipid discovery and characterization in platelets. *Circ Res* 114:1185–1203
- Helder-Jose Mendes EG, Carneiro NM, Simoes MJ, Freymuller E (2014) Morphophysiology of the paracloacal (scent) glands in females of the marsupial *Metachirus nudicaudatus*: action of estrogens. *Zoomorphology* 133:237–243
- Nilsson MA, Arnason U, Spencer PBS, Janke A (2004) Marsupial relationships and a timeline for marsupial radiation in South Gondwana. *Gene* 340:189–196
- Nilsson MA, Churakov G, Sommer M, Van Tran N, Zemann A, Brosius J, Schmitz J (2010) Tracking marsupial evolution using archaic genomic retroposon insertions. *PLoS Biol* 8:e1000436
- Bartz R, Li W-H, Venables B, Zehmer JK, Roth MR, Welti R, Anderson RGW, Liu P, Chapman KD (2007) Lipidomics reveals that adiposomes store ether lipids and mediate phospholipid traffic. *J Lipid Res* 48:837–847